AMERICAN SOCIETY FOR MICROBIOLOGY | Journal of Virology®

cis-Acting Element at the 5' Noncoding Region of Tacaribe Virus S RNA Modulates Genome Replication

Alejandra L. D'Antuono,[a] Giovanna L. Gallo,[a] Claudia Sepulveda,[b,c] Jonás Fernández,[a] Julia Brignone,[d] Graciela Gamboa,[d] Laura Riera,[d] María del Carmen Saavedra,[d] Nora López[a]

[a]Centro de Virología Humana y Animal, Consejo Nacional de Investigaciones Científicas y Técnicas—Universidad Abierta Interamericana, Buenos Aires, Argentina
[b]Laboratorio de Virología, Departamento de Química Biológica, Facultad de Ciencias Exactas y Naturales, Universidad de Buenos Aires, Buenos Aires, Argentina
[c]Instituto de Química Biológica de la Facultad de Ciencias Exactas y Naturales, Consejo Nacional de Investigaciones Científicas y Técnicas—Universidad de Buenos Aires, Buenos Aires, Argentina
[d]Instituto Nacional de Enfermedades Virales Humanas Dr. Julio I. Maiztegui, ANLIS-Malbran, Ministerio de Salud de la Nación, Pergamino, Buenos Aires, Argentina

ABSTRACT Tacaribe virus (TCRV) is the prototype of New World mammarenaviruses, a group that includes several members that cause hemorrhagic fevers in humans. The TCRV genome comprises two RNA segments, named S (small) and L (large). Both genomic segments contain noncoding regions (NCRs) at their 5′ and 3′ ends. While the 5′- and 3′-terminal 19-nucleotide sequences are known to be essential for promoter function, the role of their neighboring internal noncoding region (iNCR) sequences remains poorly understood. To analyze the relevance of the 5′ and 3′ iNCRs in TCRV S RNA synthesis, mutant S-like minigenomes and miniantigenomes were generated. Using a minireplicon assay, Northern blotting, and reverse transcription-quantitative PCR, we demonstrated that the genomic 5′ iNCR is specifically engaged in minigenome replication yet is not directly involved in minigenome transcription, and we showed that the S genome 3′ iNCR is barely engaged in this process. Analysis of partial deletions and point mutations, as well as total or partial substitution of the 5′ iNCR sequence, led us to conclude that the integrity of the whole genomic 5′ iNCR is essential and that a local predicted secondary structure or RNA-RNA interactions between the 5′ and 3′ iNCRs are not strictly required for viral S RNA synthesis. Furthermore, we employed a TCRV reverse genetic approach to ask whether manipulation of the S genomic 5′ iNCR sequence may be suitable for viral attenuation. We found that mutagenesis of the 5′ promoter-proximal subregion slightly impacted recombinant TCRV virulence *in vivo*.

IMPORTANCE The *Mammarenavirus* genus of the *Arenaviridae* family includes several members that cause severe hemorrhagic fevers associated with high morbidity and mortality rates, for which no FDA-approved vaccines and limited therapeutic resources are available. We provide evidence demonstrating the specific involvement of the TCRV S 5′ noncoding sequence adjacent to the viral promoter in replication. In addition, we examined the relevance of this region in the context of an *in vivo* infection. Our findings provide insight into the mechanism through which this 5′ viral RNA noncoding region assists the L polymerase for efficient viral S RNA synthesis. Also, these findings expand our understanding of the effect of genetic manipulation of New World mammarenavirus sequences aimed at the rational design of attenuated recombinant virus vaccine platforms.

KEYWORDS *Mammarenavirus*, Tacaribe virus, RNA replication, noncoding regions

The *Arenaviridae* family comprises enveloped viruses that infect mainly rodents (genus *Mammarenavirus*), snakes (genera *Reptarenavirus* and *Hartmanivirus*), or fish (genus *Antennavirus*) (1). Mammarenaviruses are further divided into New World (NW) and Old World (OW) groups. Tacaribe virus (TCRV) is the prototype of the NW group,

Editor Rebecca Ellis Dutch, University of Kentucky College of Medicine

Address correspondence to Nora López, noramlopar@gmail.com.

The authors declare no conflict of interest.

Received 20 January 2023
Accepted 24 January 2023

and it is the sole mammarenavirus isolated from phyllostomid bats and Lone Star ticks (2, 3). TCRV is apathogenic and is closely related to NW viruses associated with severe hemorrhagic fevers in humans, such as Junin virus (JUNV), Guanarito virus (GTOV), Machupo virus (MACV), Chapare virus (CHAPV), and Sabia virus (SABV). Other pathogenic mammarenaviruses that are classified within the OW group include Lassa virus (LASV) and lymphocytic choriomeningitis virus (LCMV) (4, 5). Because TCRV protects guinea pigs and nonhuman primates from lethal challenge with pathogenic strains of JUNV (6), it has been largely employed as a suitable model for virus-host interactions studies.

The TCRV genome is composed of two single-stranded, negative-sense RNA segments named S (small) and L (large), each comprising two open reading frames (ORFs) in opposite orientations and separated by a noncoding intergenic region (IGR). The S segment encodes the nucleocapsid protein (NP) and the precursor of the envelope glycoprotein complex (GPC). The L segment encodes the RNA-dependent RNA polymerase (L) and a RING matrix protein (Z) that is essential for viral morphogenesis (7, 8). NP encapsidates the S and L RNAs to form ribonucleoprotein complexes named nucleocapsids, which associate with the L polymerase to function as transcription-replication units. TCRV genomic S and L segments contain noncoding regions (NCRs) at their 5′ and 3′ termini whose lengths are, respectively, 68 and 76 (S) and 69 and 30 (L) nucleotides (nt). At the 5′ and 3′ ends, both S and L segments contain 19-nt sequences highly conserved across arenaviruses which are almost fully complementary to each other and that are predicted to form panhandle structures (7, 8). Transcription initiates at the 3′ end of genomic viral RNA (vRNA) and antigenomic complementary RNA (cRNA) and relies on a "cap-snatching" mechanism. In this process, the L polymerase recognizes and cleaves short capped sequences from host mRNAs to use them as primers for the synthesis of capped, nonpolyadenylated transcripts ending at the corresponding IGR (9–12). Currently available evidence supports that NP and L mRNAs are transcribed first from the vRNAs, whereas GPC and Z mRNAs are synthesized later from encapsidated cRNAs, which also act as intermediates for replication of vRNAs (13–15). Genome replication by the L protein is thought to be initiated *de novo* via a prime-and-realign mechanism, yielding a nontemplated 5′-terminal G residue at both the S and L vRNA and cRNA ends (16, 17).

For both genomic segments, the 5′- and 3′-terminal 19-nt sequences have been proven to be involved in promoter activity. Using LCMV and LASV cell-based minireplicon assays, it was initially shown that sequence specificity from residues 1 to 12 at the 3′ genomic end and sequence complementarity between the 5′ and 3′ termini along positions 13 to 19 were required for the L polymerase to mediate RNA synthesis (18, 19). Later, evidence from *in vitro* experiments demonstrated complex formation between mammarenavirus vRNA ends and L protein (16, 20–22). Moreover, binding of the MACV L protein to single-stranded 3′ vRNA promoter was shown to take place in a sequence-specific manner, with positions 2 to 5 being essential for L recruitment, while binding to single-stranded 5′ vRNA promoter was reported to occur via low-affinity interactions (20). These observations were later confirmed for LASV L protein (21). In contrast to accumulated data on the function of the terminal 19-nt promoter sequences, little is known about the contribution of their adjacent noncoding regions to viral RNA synthesis.

Here, we report evidence on the role of the 5′ and 3′ iNCRs in TCRV S RNA synthesis. Using an *in cellulo* S-like minireplicon system, we found that the genomic 5′ iNCR specifically enhanced genome replication, while it was not directly involved in transcription. In contrast, the genomic 3′ iNCR barely engaged in this process. Moreover, while the presence of the GPC coding sequence had no influence, the integrity of the 5′ iNCR was required to stimulate replication. Finally, our results revealed that although mutagenesis of the promoter-proximal subregion of the S RNA 5′ iNCR affected viral fitness in BHK-21 cells, it was associated with a low impact on virulence of recombinant TCRV *in vivo*, in a mouse model.

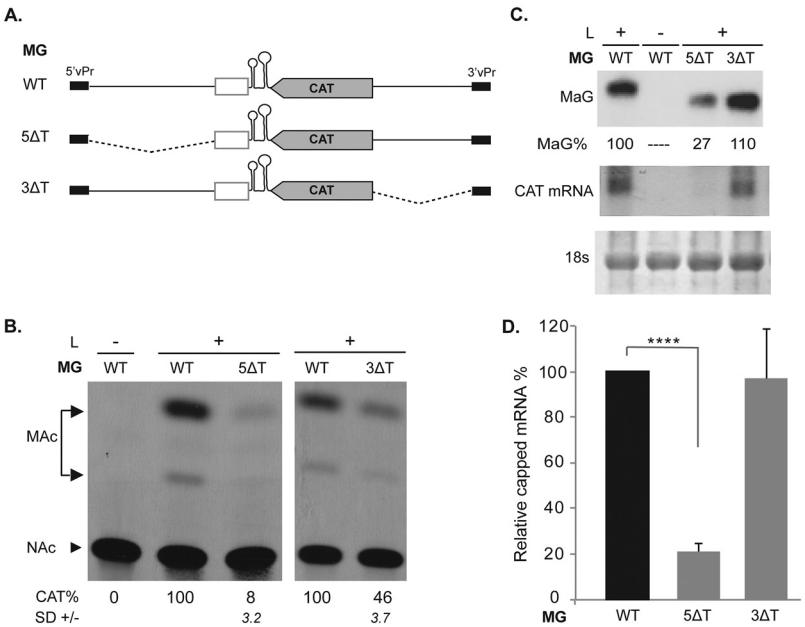

FIG 1 (A) Schematic representation of wild-type and mutant MGs carrying a complete deletion of iNCR. Wild-type (WT) MG consists of the 68-nt-long S genome 5′ NCR, followed by 171 nt of the GPC locus (empty box) plus the complete S IGR (represented as a double stem-loop), then the CAT ORF in an antisense orientation, and the complete S genome 3′ NCR (76 nt). Deleted sequences are indicated with dashes, and the 5′ and 3′ 19-nt vRNA promoter sequences (5′ vPr and 3′ vPr) are shown as black boxes. (B to D) BSR cells were transfected to express TCRV L and NP along with either wild-type or each of the indicated mutant MGs. As a negative control, the L-expressing plasmid was omitted from the transfection mix [indicated on top, L (-)]. (B) Cell extracts were prepared at 48 h posttransfection for the CAT assay. CAT values (percentages) correspond to the mean from three independent experiments and are relative to CAT levels determined for wild-type MG. Mac, monoacetylated chloramphenicol; NAc, nonacetylated chloramphenicol. (C) Total intracellular RNA was purified at 24 h posttransfection and analyzed by Northern blotting. The amount of 18S rRNA stained with ethidium bromide before blotting was used as control for gel loading (lower panel). Blots were hybridized with a ^{32}P-labeled negative-sense CAT riboprobe to detect miniantigenome (MaG) and CAT mRNA. RNA bands were visualized by autoradiography and quantified by densitometry. Results were normalized to the WT MaG levels. Data from a representative experiment are shown. (D) Capped CAT mRNA was purified at 48 h posttransfection from transfected cell lysates by immunoselection using anti-cap antibody. Purified RNA was used as the template to amplify a CAT fragment by RT-qPCR. The relative CAT RNA content was estimated as the $\Delta\Delta C_T$-based fold change (see Materials and Methods). Data represent the averages and standard deviations of 4 independent experiments, each conducted in triplicate. ****, $P < 0.0001$.

RESULTS

Role of internal noncoding sequences in viral RNA synthesis. To investigate the involvement of the 5′ and 3′ iNCRs in TCRV RNA synthesis, we first employed a well-established plasmid-driven reverse genetic system based on intracellular coexpression of TCRV NP and L proteins along with a minigenome (MG), which was a miniature version of the TCRV genomic S segment expressing the chloramphenicol acetyltransferase (CAT) reporter gene (23). In this system, the RNA-dependent RNA polymerase L synthesizes both the CAT mRNA and the full-length miniantigenome (MaG), which serves in turn as a template for multiple rounds of MG replication. On the basis of this CAT-expressing vector, mutant MGs were constructed carrying deletion of the 5′ or 3′ iNCR (Fig. 1A and Table 1) (see Materials and Methods for further details). Upon plasmid transfection in BSR cells, reporter CAT gene activity was quantified to analyze transcription-replication mediated by each mutant MG.

Results showed that CAT activity driven by the mutant 3ΔT, bearing a total deletion of the 3′ iNCR (positions 20 to 76 from the 3′ end) was about 46% of that observed for the wild-type MG, whereas deletion of the complete 5′ iNCR (positions 20 to 66 from the 5′ end; mutant 5ΔT) produced a severe impairment of reporter gene activity, evidenced by mean levels as low as 8% of those driven by the wild-type MG (Fig. 1B).

TABLE 1 Nucleotide sequences of NCRs from wild-type and mutant MGs[a]

MG	5'NCR Nucleotide Sequence (from 5' to 3', vRNA Polarity)
WT	CGCACCGGGGATCCTAGGCATTTCTTGTCCATATTTGCCTAACTGAACCAGGTGAATCACTCCCAACC*ATG*
5ΔT	CGCACCGGGGATCCTAGGC----------CCATG
5ΔP	CGCACCGGGGATCCTAGGC----------AACCAGGTGAATCACTCCCAACC*ATG*
5ΔD	CGCACCGGGGATCCTAGGCATTTCTTGTCCATATTTGCCTAACTG----------*ATG*
5ΔPp	CGCACCGGGGATCCTAGGC----------TATTTGCCTAACTGAACCAGGTGAATCACTCCCAACC*ATG*
5ΔDd	CGCACCGGGGATCCTAGGCATTTCTTGTCCATATTTGCCTAACTGAACCAGGTGAAT----------ACC*ATG*
58U	CGCACCGGGGATCCTAGGCATTTCTTGTCCATATTTGCCTAACTGAACCAGGTGAAT**TTTTTTTT**ACC*ATG*
m1	CGCACCGGGGATCCTAGGCATTTCTTGTCCAT**TAA**TGCCTAACTGAACCAGGTGAATCACTCCCAACC*ATG*
m2	CGCACCGGGGATCCTAGGCATTTCTTGTCCATATTTGCCT**TTG**TGAACCAGGTGAATCACTCCCAACC*ATG*
m3	CGCACCGGGGATCCTAGGCATTTCTTGTCCATATTTGCCTAACTGAACCAGGTG**TTA**CACTCCCAACC*ATG*
m4	CGCACCGGGGATCCTAGGCATTTC**AACAG**CATATTTGCCTAACTGAACCAGGTGAATCACTCCCAACC*ATG*
TV_P	CGCACCGGGGATCCTAGGC**TAAAGAACAGGTATAAACGGATTGACTT**CCAGGTGAATCACTCCCAACC*ATG*
TV_D	CGCACCGGGGATCCTAGGCATTTCTTGTCCATATTTGCCTAACTGAAC**AAATATGGAGAAGAAAT**ACC*ATG*
5L	CGCACCGGGGATCCTAGGC**GTTACGTGCACTCTTCTTTATTGGGCTGGATTACACAAAACTTTTCAAGC***ATG*
GTOV	CGCACAGTGGATCCTAGGC**GTTTTTACTCACGCAATAATTTGTCCACACTATTGTTGGGTGTGACCTAGCATA***ATG*
LCMV	CGCACAGTGGATCCTAGGC**TTTTTGGATTGCGCTTTCCTCCAGGTCAACTGAGTGTGGGGCTCCGTCTCGTCAGAGG***ATG*
βGlo	CGCACCGGGGATCCTAGGC**AATTTGCTTCTGACACAACTGTGTTCACTAGCAACCTCAAACAGACACC***ATG*
	3'NCR Nucleotide Sequence (from 3' to 5')
WT	GCGTGTCACCTAGGATCCGTTTAACAGATTGAGAAAGTGACTCGAGAAAAAACTTTAGGAACGAAACTAGCGGTAT*TAC*
3ΔT	GCGTGTCACCTAGGATCCG----------*TAC*

[a]Mutated nucleotide sequences are indicated with bold characters. Deleted sequences are indicated with hyphens. Italics indicate the GPC (5′ NCR) or reporter gene (3′ NCR) start codon.

In view of these observations, we asked whether deletion of the 5′ iNCR specifically affected genomic and antigenomic RNA synthesis and, in turn, resulted in decreased reporter mRNA accumulation, or whether it was only associated with an impairment of CAT mRNA transcription. To answer this question, total RNA from transfected cells was analyzed by Northern blotting using a negative-sense CAT riboprobe (Fig. 1C). As expected, neither MaG nor CAT mRNA was detected upon omission of the L-expressing plasmid from the transfection mix. Densitometric quantification of bands indicated that complete deletion of the 3′ iNCR (3ΔT) did not substantially affect MaG levels, whereas a marked reduction of MaG accumulation was observed in cells expressing the 5′ iNCR-deleted MG (5ΔT) compared with control cells expressing wild-type MG (Fig. 1C). Because the band corresponding to CAT mRNA was diffuse, we employed an alternative approach to quantify this RNA species. Lysates from transfected cell monolayers were immunoselected with anti-cap antibodies, and the amount of nonencapsidated, capped CAT mRNA was determined by reverse transcription-quantitative PCR (RT-qPCR) (Fig. 1D). These experiments confirmed that removal of the 3′ iNCR had little impact on CAT mRNA accumulation, while deletion of the 5′ iNCR dramatically reduced the amounts of CAT mRNA to levels consistent with the decreased levels of mutant MaG, as detected by Northern blotting (Fig. 1C). Likewise, quantification of NP-encapsidated MG RNA by immunoselection with anti-NP antibodies followed by RT-qPCR confirmed that, while MG3ΔT RNA accumulated at wild-type levels, accumulation of encapsidated mutant MG5ΔT RNA was profoundly reduced compared to wild-type MG (data not shown).

Overall, these results clearly indicated that deletion of the iNCR proximal to the 5′ vRNA promoter abrogated MG replication and, consequently, impacted mRNA CAT transcription. Thus, these findings suggested that TCRV S genomic 5′ iNCR harbors a key element(s) required for viral RNA replication.

To get additional insight on the relevance of the iNCRs in viral RNA synthesis, we created a firefly luciferase (FLUC)-expressing TCRV S-like MaG and derivative mutants bearing total deletion of either the 5′ or the 3′ iNCR (see Materials and Methods) (Table 2 and Fig. 2A, left). Wild-type and mutant MaGs were tested for their ability to support FLUC expression (Fig. 2A, right). Results revealed that, while FLUC activity was almost unaffected by total deletion of the antigenomic 5′ iNCR (5ΔT), it was highly reduced by deletion of the complete antigenomic 3′ iNCR (3ΔT). These results strongly supported the notion that the genomic 5′ iNCR and/or the antigenomic 3′ iNCR contained a crucial signal(s) for viral replication.

TABLE 2 Nucleotide sequences of NCR from wild-type and mutant MaGs[a]

MaG	5'NCR Nucleotide Sequence (from 5' to 3', vcRNA Polarity)
WT	CGCACAGTGGATCCTAGGCAAATTGTCTAACTCTTTCACTGAGCTCTTTTTTGAAATCCTTGCTTTGATCGCCATAC*CTAGAT*
5ΔT	CGCACAGTGGATCCTAGGC----------*CTAGAT*
	3'NCR Nucleotide Sequence (from 3' to 5')
WT	GCGTGGCCCCTAGGATCCGTAAAGAACAGGTATAAACGGATTGACTTGGTCCACTTAGTGAGGGTTGG*TAC*
3ΔT	GCGTGTCACCTAGGATCCG----------TGG*TAC*

[a]Deleted sequences are indicated with hyphens. Italics indicate the linker sequence (5′ NCR) or reporter gene (3′ NCR) start codon.

To deepen knowledge and delimit the sequences within the genomic 5′ iNCR required for replication, we rationally designed a series of deletion mutants based on a FLUC-expressing MG (see Materials and Methods) (Table 1). These new constructions were tested for their ability to sustain reporter gene expression upon cell cotransfection with the NP- and L-expressing plasmids. As previously observed (Fig. 1), deletion of the entire 5′ iNCR (mutant 5ΔT) resulted in a strong reduction (85%) of reporter gene activity, compared with FLUC activity levels driven by wild-type MG (Fig. 2B). Similarly reduced levels of FLUC expression were observed when partial deletions were evaluated, regardless of the length or location within the 5′ iNCR. The removal of positions 20 to 45 (5ΔP) or 20 to 31 (5ΔPp), located next to the 5′ vRNA promoter, as well as deletion of distal sequences spanning residues 46 to 68 (5ΔD) or 58 to 65 (5ΔDd), decreased reporter gene expression to mean levels ranging between 15 and 27% of those observed for wild-type MG (Fig. 2B and C, right). Comparable results were obtained when the central subregion of the iNCR was deleted (positions 32 to 58 from the 5′ end) (data not shown). These results suggested that the full length of the 5′ iNCR may be relevant for viral replication. This conclusion was further supported by the fact that mutant 5U8, in which positions 58 to 65 (deleted in mutant 5ΔDd) were replaced with U residues to restore the 5′ iNCR length, directed average levels of FLUC activity that increased to 64% of those driven by the wild-type MG (Fig. 2B).

To assess whether the coding sequence neighboring the 5′iNCR could modulate viral RNA replication and/or transcription, we designed a new MG (WT_G), which included the complete GPC sequence, and thus more closely resembled the TCRV S genome. In addition, we constructed mutant 5ΔPp_G, also containing the GPC sequence, and a control MG (WT_UN), which included an unrelated sequence of similar size (1,300 bp) at the GPC locus (Fig. 2C). Both WT_G and 5ΔPp_G exhibited a slightly reduced capacity to express FLUC, compared with WT MG and 5ΔPp, respectively. In addition, control WT_UN directed levels of FLUC activity that did not significantly differ from those driven by WT_G (Fig. 2C). Thus, the presence of the GPC coding sequence did not stimulate MG replication and/or translation in any case, indicating that the GPC sequence is not critically involved in viral RNA synthesis regulation. Altogether, these data confirmed the engagement of genomic 5′ iNCR in viral replication and suggested that the full length of this genome region may be required to preserve the integrity of the putative signal(s) involved.

Based on our findings, we then asked whether the S genome 5′ iNCR could contain *cis*-acting structural elements engaged in viral replication. The predicted folding of the terminal TCRV S NCRs displayed the 19-nt terminal panhandle structure and a second stretch involving 5′-to-3′ base-pairing that spanned positions 25 to 29 from the 5′ end (Fig. 3A). The structure showed additional double-stranded stretches within the 5′ iNCR, with positions 33 to 40 and 50 to 57 conforming the stem of a predicted hairpin structure (Fig. 3A, SL1). In order to evaluate a possible role of the predicted structure in viral RNA synthesis, three substitution mutants (m1 to m3) with changes in key positions within SL1 were designed. In addition, the sequence spanning positions 25 to 29 (UUGUC), which was predicted to base-pair with the 3′ iNCR, was replaced by its complementary sequence to obtain mutant m4 (Fig. 3A). Then, mutant MGs were tested for their ability to drive reporter gene expression in the MG assay. The results showed

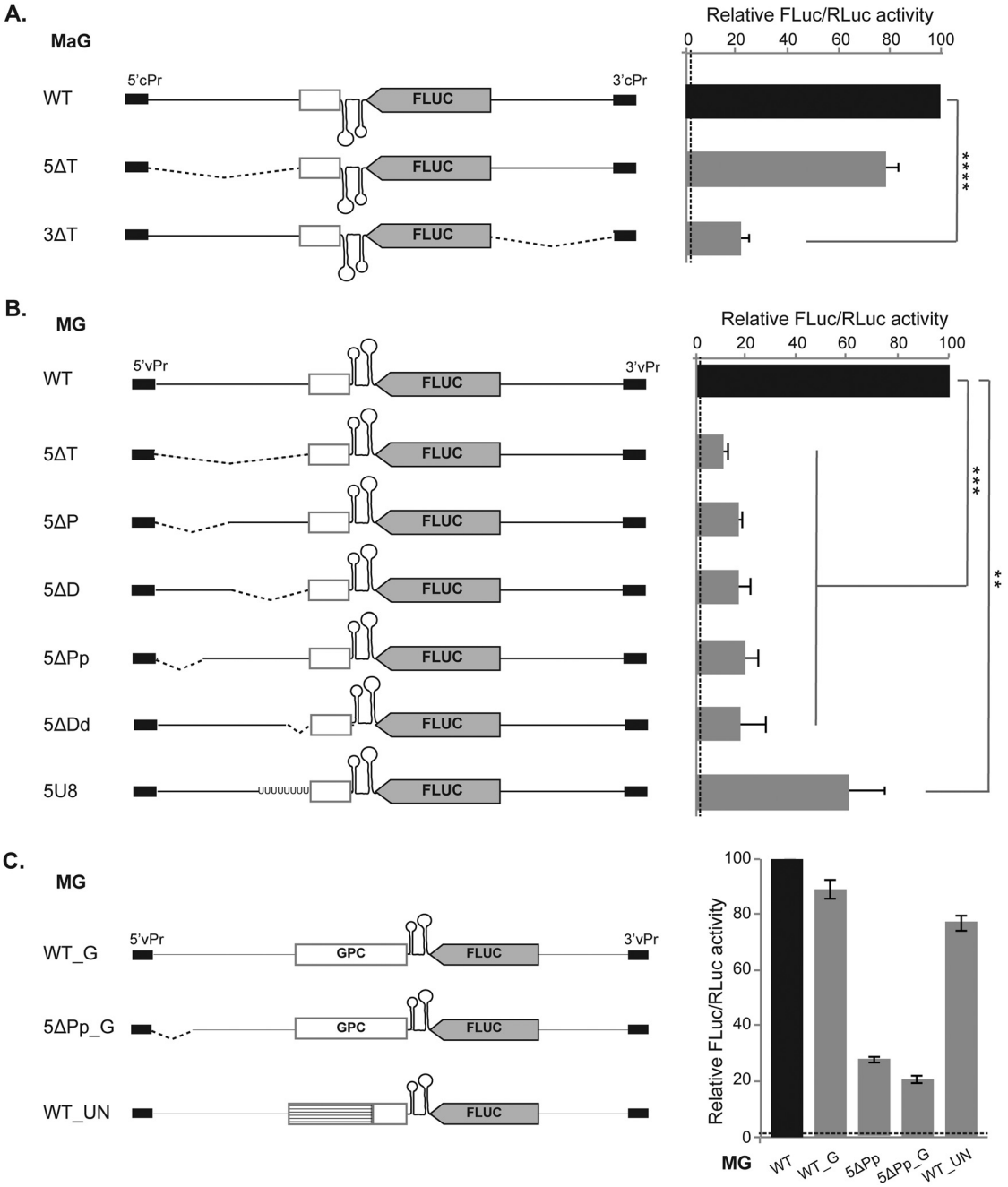

FIG 2 (Left) Schematic representation (not to scale) of the wild-type and mutant versions of FLUC-expressing MaG (A) or MG (B and C). Deleted sequences are indicated with dashes, and the 5′ and 3′ 19-nt cRNA (cPr) and vRNA (vPr) promoter sequences are shown as black boxes. The empty box represents partial (A and B) or total (C) GPC coding sequence, and the striped box (C) corresponds to an unrelated, nonviral sequence. (Right) BSR cells were transfected to express TCRV L, TCRV NP, and either WT or each of the indicated mutant MaG (A) or MG (B and C). Transfection efficiency was monitored by addition of the renilla luciferase (RLUC) reporter vector phRL-TK to the transfection mixture. FLUC activity was determined at 48 h posttransfection in cell lysates, as described in Materials and Methods. Values shown correspond to the means from at least three independent experiments and are normalized to FLUC activity determined for the wild-type MaG (A) or MG (B and C), set as 100%. **, $P \leq 0.01$; ***, $P \leq 0.001$; ****, $P \leq 0.0001$. Mean relative FLUC activity levels, determined for cell monolayers expressing MG WT and NP in the absence of L (negative control), are indicated with a dotted line.

that mutations that would destabilize the SL1 stem (ATT to TAA [m1] or AAT to TTA [m3]) resulted in levels of FLUC activity that ranged between 91 and 93% of those directed by the wild-type MG. Similar results were obtained for control mutant m2, carrying changes of three residues at the SL1 loop (AAC to TTG) (Fig. 3B). These

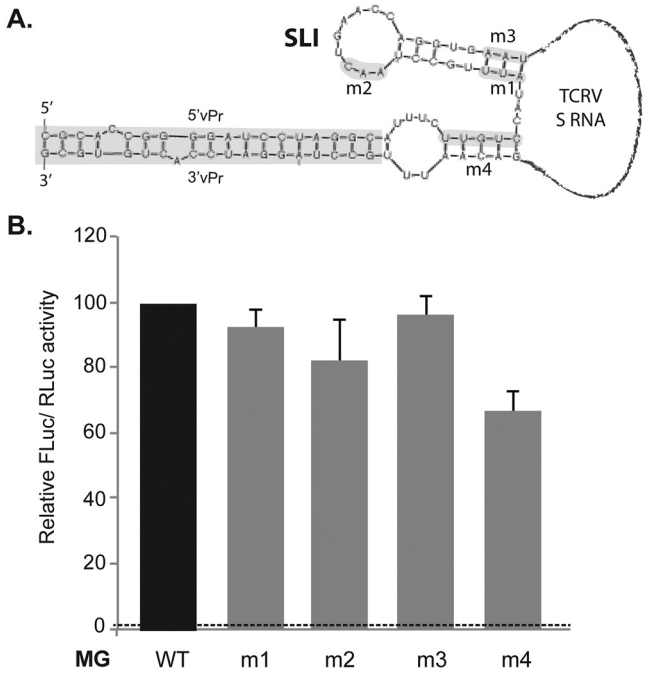

FIG 3 (A) Predicted secondary structure of the TCRV S RNA 5′ and 3′ noncoding sequences, obtained by using the RNAfold web server (http://rna.tbi.univie.ac.at/cgi-bin/RNAWebSuite/RNAfold.cgi). For the analysis, the 5′ and 3′ NCRs were linked with a track of A residues; coding and intergenic sequences were omitted. The 5′ and 3′ 19-nt vRNA promoter (vPr) and positions that were changed to generate mutant MGs m1 to m4 are indicated in gray. (B) BSR cells were transfected to express TCRV L and NP and either WT or each of the indicated mutant MGs. FLUC activity was determined at 48 h posttransfection in cell lysates, as described for Fig. 2. Values correspond to the means from at least three independent experiments and are expressed as the percentage of wild-type MG, set as 100%. The mean relative FLUC activity level determined for negative-control cell monolayers is indicated with a dotted line.

observations indicated that the predicted SL1 structure may not play a central role in viral RNA synthesis. On the other hand, mutation of the UUGUC sequence resulted in mean levels of FLUC activity about 71% of those observed for the wild-type MG (Fig. 3B). These results, along with the finding that the impact of deletions at the 5′ iNCR had a significantly different effect than similar deletions at the 3′ iNCR, in the context of both MG and MaG (Fig. 2), supported the idea that RNA-RNA interactions between the 5′ and 3′ iNCRs may be not strictly required for viral RNA synthesis.

Next, we aimed to study the nature of the signals within the genomic S segment 5′ iNCR that are important for viral RNA synthesis. To obtain insights into this, we constructed mutant MGs bearing complete substitutions of this region (Table 1) (see Materials and Methods) and assayed them for their ability to mediate FLUC activity upon coexpression with NP and L proteins in mammalian cells (Fig. 4). Replacement of the S RNA 5′ iNCR (49 nt) with the corresponding sequence from a closely related NW mammarenavirus, such as GTOV (54 nt) or the 5′ iNCR sequence from the TCRV L genomic segment (50 nt; mutant 5L), did not significantly affect MG expression levels. A statistically significant reduction of FLUC expression, in comparison to wild-type MG, was observed when the region was changed by the S RNA 5′ iNCR from the phylogenetically more distant OW LCMV (58 nt long). This evidence suggested that a common signal(s) resident at the genomic 5′ iNCR could possibly operate to sustain synthesis of clade B mammarenavirus S and L RNAs. Notably, when a 49-nt-long, nonrelated sequence from the 5′ untranslated region of human globin mRNA was substituted for the TCRV S 5′ iNCR to generate mutant βGlo, levels of reporter gene expression did not differ significantly from those directed by the wild-type MG. These results suggested that the substituting sequences in these replication-competent MGs, which

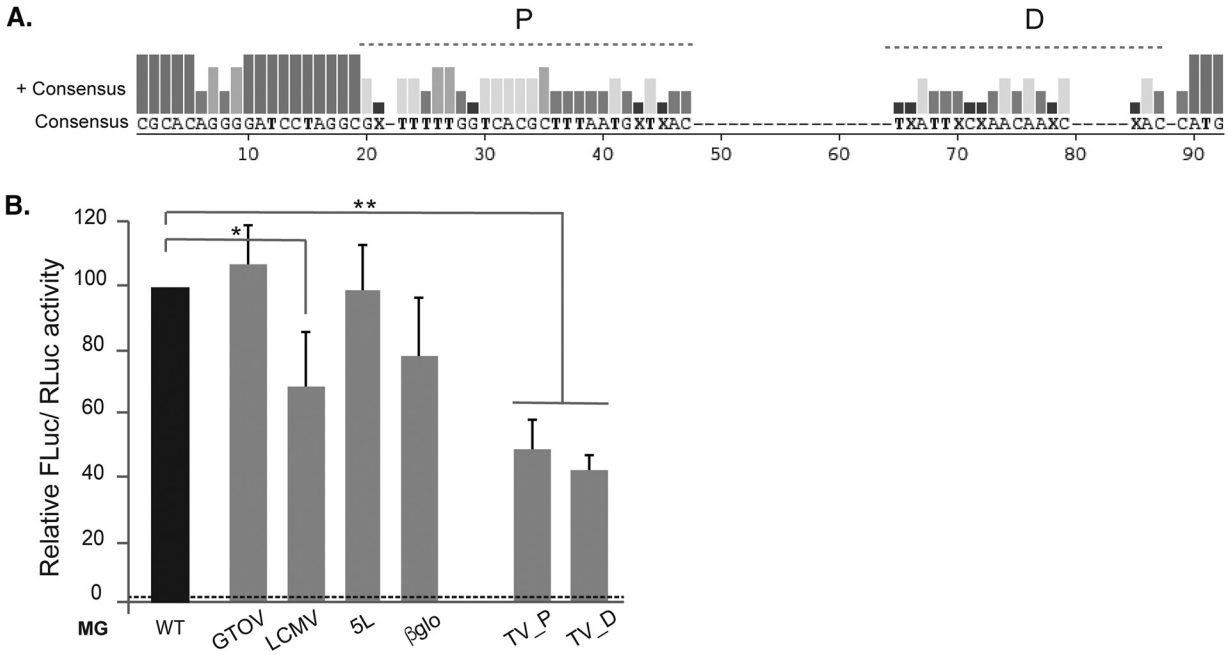

FIG 4 (A) Comparison of the 5′ NCR from TCRV S RNA, mutant MGs, and clade B mammarenaviruses. The sequences from the wild-type and substitution mutant MGs (5L, GTOV, βGlo) (Table 1) and from the S RNA 5′ NCR of CHAPV (NC_010562.1), SABV (NC_006317.1), MACV (NC_005078.1), JUNV (NC_005081.1), Cupixi virus (NC_010254.1), and Amapari virus (NC_010247.1) were aligned using the ClustalW algorithm included in the MegAlign program (DNASTAR, Madison, WI, USA). The promoter-proximal (P) and promoter-distal (D) subregions are indicated. (B) BSR cells were transfected to express TCRV L, TCRV NP, and either wild-type or each of the indicated mutant MGs. FLUC activity was determined at 48 h posttransfection in cell lysates, as described for Fig. 2. The dotted line shows the mean relative FLUC activity level determined for negative-control cell monolayers, expressing MG WT plus NP (in the absence of L). Values correspond to the means of at least three independent experiments and were normalized to FLUC activity determined for the wild-type MG. *, $P \leq 0.05$; **, $P \leq 0.01$.

displayed variable degrees of sequence identity with the TCRV S 5′ iNCR, could either harbor a relevant motif(s) or, alternatively, they could provide the steric arrangement necessary to sustain MG replication. Comparison of the 5′ NCR sequences from wild-type and mutant MGs with the S genomic 5′ NCR from several clade B mammarenaviruses, in our search for common elements, revealed no obvious consensus sequence motifs. Instead, it led to the recognition of a promoter-proximal subregion (positions 20 to 47 from the 5′ end in TCRV S RNA) (Fig. 4A), which displayed a high U/C content (59% to 77%) and was well conserved among clade B mammarenavirus S RNA (24). To assess whether this promoter-proximal subregion may contain a signal(s) engaged in viral RNA synthesis, additional substitution mutants were designed. Thus, the wild-type sequence comprising positions 20 to 47 was changed to its complementary sequence to generate mutant TV_P (Table 1) (see Materials and Methods). As a control, we generated mutant TV_D, by replacement of the promoter-distal sequence (residues 48 to 65) with a sequence of similar base composition as the substituting sequence in mutant TV_P (24% U/C) (Table 1). The results showed that both TV_P and TV_D elicited FLUC expression levels that dropped to nearly 50% of those driven by the wild-type MG, highlighting the importance of both subregions for viral RNA synthesis (Fig. 4B).

Impact of the S genomic 5′ iNCR on recombinant TCRV virulence. We previously developed a reverse genetic system to rescue recombinant TCRV (rTCRV). Using this system, we generated a mutant rTCRV (rTCRVsNCR) bearing the TV_P mutation (transversion substitution of positions 20 to 47) within the S vRNA 5′ NCR, which appeared to display an altered fitness in baby hamster kidney fibroblasts (BHK-21 cells) compared with wild-type rTCRV (24). In view of this precedent and our results showing that mutant MG TV_P exhibited a reduced capacity to drive FLUC expression (Fig. 4), we sought to explore whether the conserved S genomic promoter-proximal region could be a suitable target for NW mammarenavirus attenuation *in vivo*.

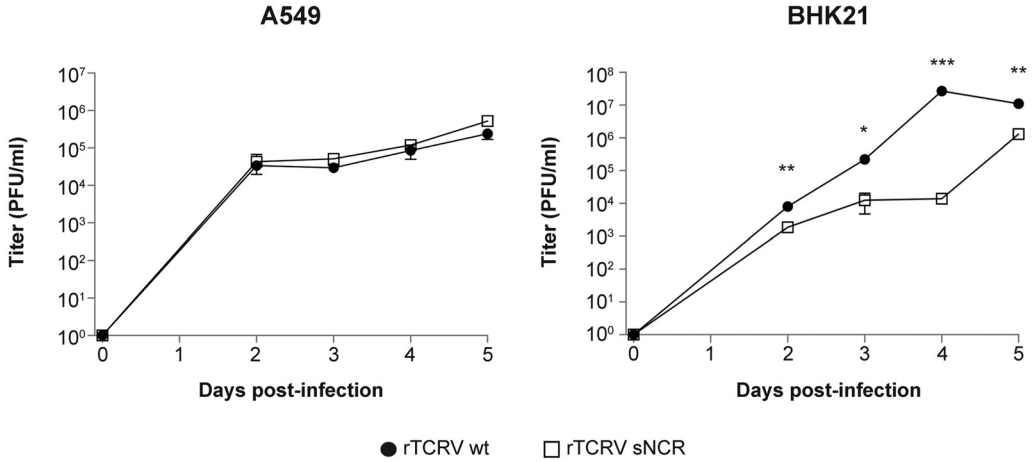

FIG 5 Viral growth kinetics. BHK-21 or A549 cells were infected with wild-type rTCRV or mutant rTCRVsNCR at an MOI of 0.001 PFU/cell. Aliquots of cell supernatants were collected daily, and virus was titrated by standard plaque assay on Vero cells. Each point corresponds to the average of triplicate wells (± SD). A representative of three independent experiments is shown. *, $P \leq 0.05$; **, $P \leq 0.01$; ***, $P \leq 0.001$.

First, to further support our previous observations, the growth of wild-type rTCRV and mutant rTCRVsNCR was assessed both in BHK-21 cells and in a human epithelial cell line (A549) commonly employed in arenavirus studies. The results confirmed that the mutant virus displayed a significantly lower growth capacity than wild-type rTCRV in BHK-21 cells. In contrast, both viruses exhibited similar growth kinetics in human A549 cells (Fig. 5).

Next, we evaluated viral virulence in a well-established newborn mouse TCRV infection model. Groups of 2-day-old BALB/cJ mice (n = 10/group) were inoculated intracranially with 10-fold serial dilutions, ranging from 1 to 10^3 PFU/animal, of the wild-type rTCRV or mutant rTCRVsNCR. As negative controls, groups of mice (n = 10) were inoculated with medium alone or left untreated. Mortality was monitored daily over a 21-day period. As expected, both control groups survived through day 21, when the experiment was terminated. Wild-type rTCRV and mutant rTCRVsNCR were highly virulent in suckling mice, causing mostly 100% mortality, with only one survivor recorded for the group inoculated with 100 PFU of rTCRVsNCR. However, minor differences in time to death were observed, predominantly for mice inoculated with 1,000, 100, or 10 PFU, as survival curves for the mutant virus were slightly delayed compared with those for wild-type rTCRV-inoculated mice (Fig. 6A). To evaluate virus dissemination, two animals per group were sacrificed at day 8 postinoculation. Brain, liver, and spleen were collected, and viral load was determined by plaque assay. No infectious virus was detected in liver or spleen, while high virus loads were observed in brains of either wild-type or mutant rTCRV-inoculated mice. However, animals infected with wild-type rTCRV exhibited average viral titers somewhat higher than those of mutant rTCRVsNCR-infected animals (Fig. 6B). Nevertheless, the virus dose required to cause 50% mortality (LD_{50}) was estimated to be $<$1 PFU for both wild-type rTCRV and rTCRVsNCR. These results indicated that, in spite of causing a 50% reduction in MG replication *in cellulo* and lower viral fitness in BHK-21 cells, mutagenesis of the 5′ iNCR promoter-proximal region of the S genomic RNA only slightly impacted rTCRV virulence *in vivo*.

DISCUSSION

The role of the 5′- and 3′-terminal 19-nt vRNA sequences in promoting arenavirus RNA replication has been deeply characterized. However, much less is known about the function of 5′ and 3′ internal noncoding regions, which separate the terminal promoter from viral coding sequences. To get insight into this question, we employed a TCRV cell-based replicon system that capitulated viral transcription and replication processes. Analysis of mutant S-like minigenomes or miniantigenomes carrying a

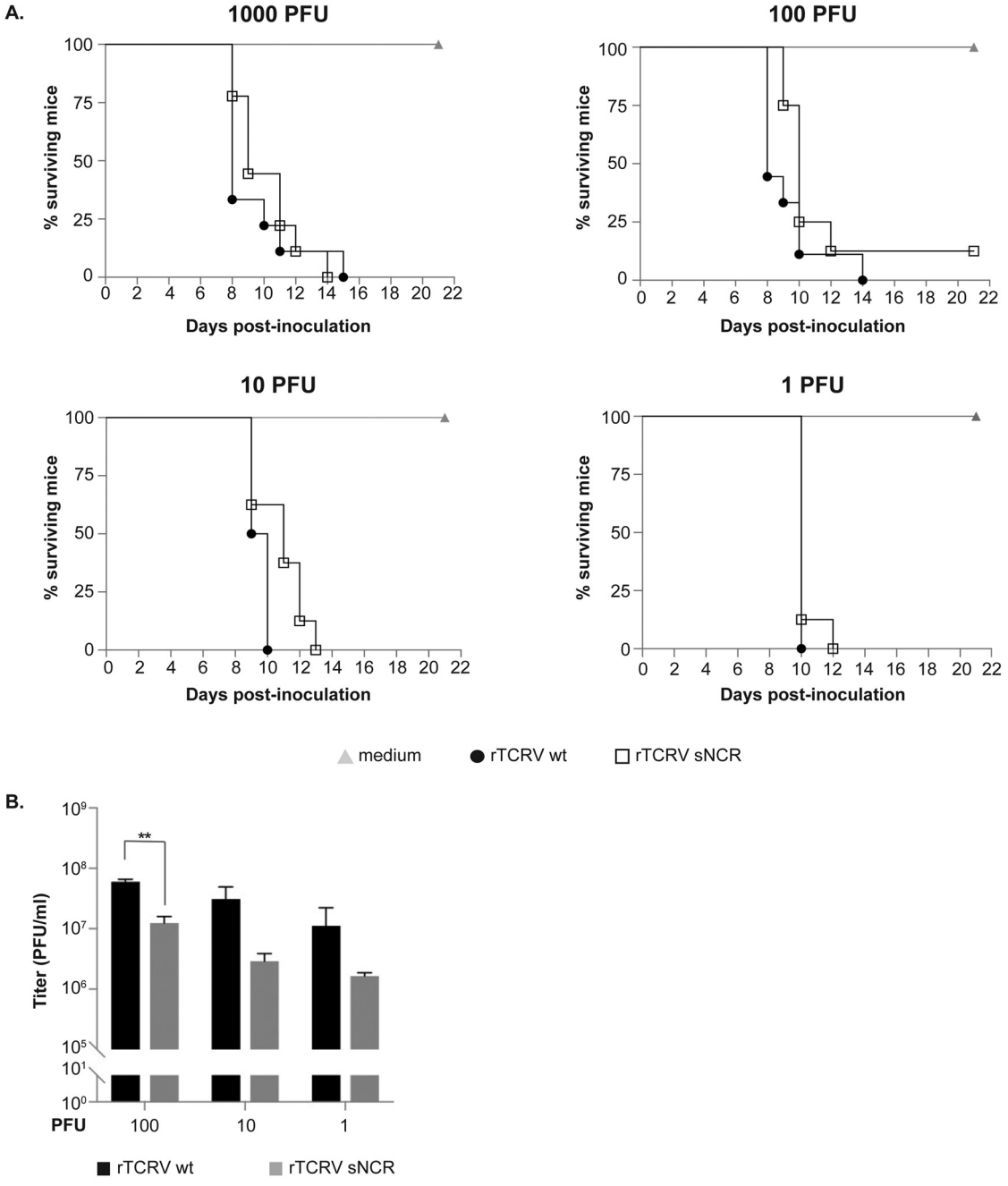

FIG 6 (A) Survival curves. Groups of mice were inoculated intracranially with the indicated amounts of wild-type rTCRV or mutant rTCRVsNCR. Mortality was monitored daily for 21 days. (B) Viral titers in brain tissue of infected animals. Two mice per group were sacrificed at 8 days postinoculation. Brains were weighed and homogenized in serum-free medium. Viral titers were determined by plaque assay on Vero cells. Values correspond to the means (± SD) of triplicate assays per animal. **, $P \leq 0.01$.

deletion within the 3′ or 5′ iNCR indicated that relevant signals for viral RNA synthesis likely reside in the genomic 5′ iNCR and/or the antigenomic 3′ iNCR. In accordance with these findings, previous studies had reported that reduced levels of LCMV S-like MG RNA accumulation or of MG-directed reporter gene expression were associated with deletion within the 5′ iNCR (19, 25). Likewise, the growth efficiency of recombinant LASV was affected by deletions within the genomic S RNA 5′ iNCR to a higher extent than deletions within the 3′ iNCR (26).

Importantly, our data from Northern blotting and RT-qPCR analyses (Fig. 1) demonstrated that the genomic 5′ iNCR is specifically engaged in RNA replication. Moreover,

while the GPC coding sequence appears to have no impact, preservation of the iNCR's full length is a requirement for this region to assist in RNA synthesis (Fig. 2). This raised the question of the possible involvement of a local secondary structure in viral RNA synthesis. However, mutagenesis of nucleotides stabilizing the predicted folding into a stem-loop (SL1) had little effect on MG expression (mutants m1 and m3) (Fig. 3). This suggested that SL1 structure may be irrelevant for viral RNA synthesis. Nevertheless, considering that the viral RNAs associate with the nucleocapsid protein, possible transient RNA structures may differ from those theoretically achieved on the assumption of naked RNA and the possibility that the S 5′ vRNA iNCR folds into a putative local structure(s) other than those predicted cannot be discarded.

Our findings also revealed that the GTOV S vRNA 5' iNCR, as well as the TCRV L vRNA 5′ iNCR, can functionally replace the corresponding sequence in the TCRV S segment analog, while change to the S vRNA 5′ iNCR from LCMV resulted in somewhat decreased MG expression (Fig. 4), suggesting that a common element(s) might operate to stimulate replication of clade B mammarenavirus S and L segments. Surprisingly, however, the TCRV S vRNA 5′ iNCR could also be replaced by a nonrelated sequence (βGlo) without a detectable impact on MG replication. Furthermore, mutation of the U/C-rich 5′ promoter-proximal subregion (TV_P), which included positions well conserved among clade B mammarenaviruses, as well as substitution of the promoter-distal subregion (TV_D), significantly reduced reporter gene expression (Fig. 4). Overall, our results support the notion that not only the full length of the S genomic 5′ iNCR is required, but also that the sequences of both the promoter-proximal and the promoter-distal subregions are important for viral replication. In contrast, for LCMV, it has been reported that while the subregion spanning nt 20 to 40 is essential, deletion of distal positions within the 5′ iNCR has no impact on S-like minigenome expression. In addition, it has been suggested that the predicted panhandle structure comprising part of the 5′ and 3′ iNCRs could be involved in the recognition by the L protein (25). Interestingly, the internal panhandle structure appears to play a minor role in TCRV S RNA replication, as suggested by the observation that total deletion of the genomic 3′ iNCR (Fig. 1 and 2), or substitution of positions within the genomic 5′ iNCR that are predicted to base-pair with the 3′ iNCR (UUGUC, m4) (Fig. 3) barely affected MG replication. These findings expanded our understanding of the differences between New World and Old World mammarenaviruses.

Structural studies on other segmented negative-stranded RNA viruses, such as influenza virus and La Crosse orthobunyavirus, have revealed that the 5′ and 3′ vRNA promoters bind as a single strain on separated binding sites of the viral polymerase. Moreover, binding of the 5′ vRNA promoter as a stem-loop structure has been associated with structural organization of the active site and allosteric activation of the polymerase (27–29). In the case of arenaviruses, recent evidence has indicated that binding of the 5′ genomic and antigenomic termini enhances the enzymatic activity of MACV and LASV L polymerases (16, 22, 30). Moreover, structural analyses have shown the bound promoter at the LASV L protein, with nucleotides 0 to 9 of the 5′ end forming a compact hook structure (22). In addition, mutation of the 5′ binding site of L protein has been reported to impair polymerase activity in a LASV minireplicon system (22). Based on the currently available evidence, a model has been proposed in which the L polymerase initially binds the double-stranded 19-nt promoter and melts the panhandle to position single-stranded 5′ and 3′ termini for initiation (16, 20–22, 30). The 5′ end of the nascent RNA folds into a hook-like structure, similar to that described for influenza and La Crosse viruses, which would bind free L to assemble a preactivated polymerase complex (16, 30). In light of this model, and considering the evidence reported here, we can hypothesize that binding of the structured 5′ vRNA promoter to the L polymerase may be assisted by the neighboring genomic iNCR, either through a direct interaction with the L protein or because the 5′ iNCR is required for stabilization of the 5' vRNA promoter-L protein complex. In any case, mutation of the 5′ iNCR would hamper the interaction between the polymerase and the 5′ end of the vRNA template, thereby abrogating allosteric activation. Alternatively, the 5′ vRNA iNCR might participate

in coupling to host factors involved in polymerase complex assembly or in encapsidation of the nascent RNA strand by NP. Further studies using *in vitro* encapsidation and replication assays will elucidate how the genomic 5′ iNCR interacts with the polymerase complex to assist in viral RNA synthesis.

Viral genome noncoding sequences have been explored as a target to generate recombinant attenuated viral variants (31). Precisely, the S segment 5′ and 3′ iNCRs of the OW LCMV and LASV have been implicated in virulence in mice (25, 26). Considering our finding that the S genomic 5′ iNCR specifically impacted viral RNA replication, we employed the reverse genetic approach to ask whether mutagenesis of the conserved promoter-proximal subregion may represent an *in vivo* viral attenuation determinant. We first confirmed that the TV_P mutation reduced the growth capacity of mutant rTCRVsNCR in BHK-21 cells, compared with wild-type rTCRV (Fig. 5). Despite that, our results showed that the TV_P mutation of the S genomic 5′ iNCR had little impact on viral virulence in mice. To explain the apparent discrepancy between these results, it could be considered current evidence indicating that a higher proportion of S vRNA over L vRNA accumulates both in purified virions and in mammarenavirus-infected cells, during acute and persistent infections (14, 32–34). In particular, higher S-to-L ratios have been detected in TCRV viral stocks after several passages at a high multiplicity of infection (MOI) in cell culture, compared with stocks obtained after infection at a low MOI with cloned viruses (35). It is plausible that decreased levels of S RNA synthesis during *in vivo* infection with mutant rTCRVsNCR, as can be expected according to the diminished capacity of mutant MG TV_P to replicate in our minireplicon assay, may be insufficient to result in reduced viral yields. Further examination is needed to depict whether interaction of the mutant virus with different cell types may modulate the infection outcome.

MATERIALS AND METHODS

Cells. African green monkey kidney (Vero) and human lung epithelial A549 cells were maintained in Dulbecco's modified Eagle's medium (Invitrogen). Baby hamster kidney cells (BHK-21), BSR cells (a clone of BHK-21), and BHK-T7/9 cells stably expressing the T7 RNA polymerase (36) were grown in Glasgow minimum essential medium (Invitrogen). Growth medium was supplemented with 10% fetal calf serum (Invitrogen) and penicillin (100 U/mL)–streptomycin (100 μg/mL) (Invitrogen).

Recombinant viruses. Generation of wild-type recombinant TCRV (rTRCV) and mutant rTCRVsNCR was previously described (24). Briefly, subconfluent monolayers of BHK/T7-9 cells were transfected with pLag, pTCRV L, and wild-type pSag or mutant pSagsNCR (see below). At 6 days posttransfection, supernatants were collected (P0), clarified by low-speed centrifugation, and stored at −85°C. Recombinant viruses were amplified by infection of BHK-21 cell monolayers with P0 at an MOI of 0.005. Supernatants were collected at day 7 postinfection and titrated by standard plaque assay on Vero cells (37).

Plasmids. Plasmids pTCRV N and pTCRV L, which express TCRV NP and L proteins, respectively, under the control of the T7 RNA polymerase promoter, and plasmid pS-CAT, expressing a TCRV genomic S RNA analog under the control of the murine polymerase I promoter, were previously generated (23). Plasmids pSag and pLag, expressing the full-length antigenomic copies of TCRV S and L RNAs, respectively, and mutant plasmid pSagsNCR, containing a transversion of positions 20 to 47 from the S genome 5′ end, were previously obtained (24).

Plasmid pMGFLUC was previously generated by replacing the CAT ORF with the firefly luciferase (FLUC) coding sequence into pS-CAT (38).

Plasmids pMaGCAT and pMaGFLUC directed the synthesis of RNA analogs to the TCRV antigenomic sense S RNA, which expressed the CAT and FLUC reporter genes, respectively, under the T7 RNA polymerase promoter control. To generate plasmid pMaGCAT, a DNA fragment spanning positions 1493 to 1940 (447 bp) of the TCRV S RNA was obtained by digestion of p2b2 (13) with BstXI and XbaI. The fragment was subcloned into the SnaBI site of plasmid pAgenCAT (39). To construct plasmid pMaGFLUC, a DNA fragment comprising the FLUC ORF was generated by standard PCR and cloned between SfiI and NcoI sites into pMaGCAT. Thus, plasmid pMaGFLUC comprised (5′ to 3′) the entire TCRV S antigenome 5′ noncoding sequence, a 307-bp linker sequence (positions 1940 to 1633 of the S RNA), the antigenomic sense S RNA IGR, a 23-bp spacer (positions 1516 to 1493 of the S RNA), the FLUC reporter gene ORF in an antisense orientation, and the complete S antigenome 3′ NCR.

Plasmids expressing mutant MGs and MaGs. Total or partial deletions were first introduced into plasmid pS-CAT by overlap extension PCR. Restriction sites ApaI and SfiI or EcoRI and PstI were used to replace the wild-type sequence by the deleted fragment into the genomic 5′ and 3′ iNCR, respectively. Then, to replace the CAT ORF by the FLUC coding sequence in each of the mutant plasmids, the fragment between the SacI and BsaAI restriction sites was swapped with the SacI-BsaAI fragment from pMGFLUC.

Overlap extension PCR was also employed to introduce deletions into the MaG iNCRs, using plasmid pMaGFLUC as the template. Unique restriction sites AlwNI and DraIII or EcoRI and PstI were used to substitute the wild-type sequence for the deleted fragment into 5′ iNCR and 3′ iNCR, respectively.

Point mutations were introduced by site-directed mutagenesis, using the QuikChange site-directed mutagenesis kit (Agilent Technologies), with pMGFLUC as the template and primers containing the mutated sequences.

In order to construct mutant minigenomes carrying partial or complete substitution of the 5′ iNCR, a BamHI site at position 9 within the 5′ NCR was changed to a KpnI site in plasmid pMGFLUC by site-directed mutagenesis. Wild-type 5′ iNCR was replaced by the corresponding mutant synthetic DNA fragment (provided by IDT Corporation) after digestion of pMGFLUC with KpnI and NcoI. The KpnI site was then changed back to the wild-type sequence by site-directed mutagenesis.

To obtain the plasmids expressing MGs WT_G and 5ΔPp_G (Fig. 2C), a fragment corresponding to positions 1 to 1512 of the TCRV GPC coding sequence, obtained by digestion of pTM1-GPC (23) with NcoI and AccI, was cloned between the NcoI and BstXI sites of pMGFLUC and the mutant 5ΔPp-expressing plasmid, respectively, by standard methods. To generate the mutant WT_UN-encoding plasmid, a 1,300-bp fragment obtained after digestion of plasmid pEGFP (InvivoGen) with NcoI was inserted into the NcoI site of pMGFLUC. Thus, MG WT_UN comprised a nonviral 1,300-nt sequence flanked by the 5′ vRNA iNCR and a 171-nt sequence of the 3′-terminal region of the GPC locus.

Plasmid pCMV-T7pol expresses the bacteriophage T7 RNA polymerase under the control of the cytomegalovirus promoter (40) and was kindly provided by Martin A. Billeter (University of Zurich, Irchel, Switzerland).

All plasmids were purified by using the Qiagen Tip-100 system (Qiagen Inc., Valencia, CA). All constructs were completely verified by dideoxynucleotide double-strand DNA sequencing (Macrogen Inc.).

Sequences of the 5′ and 3′ NCR of wild-type and mutant MGs or MaGs are provided in Tables 1 and 2.

Minireplicon assay. BSR cells grown in 24-well dishes were transfected (per well) with 0.5 μg of pTCRV L and 1 μg of the TCRV NP-expressing plasmid along with 1 μg of the indicated MG- or MaG-expressing plasmid, using Lipofectamine 2000 (Invitrogen) as previously described (38). Synthesis of NP and L from pTCRV-NP and pTCRV-L, as well as wild-type and mutant CAT-expressing MGs, was driven by the T7 RNA polymerase supplied *in trans* by cotransfection of 0.5 μg of pCMV-T7pol. The total amount per well of transfected DNA was kept constant by the addition of empty pTM1 DNA vector. When FLUC was used as the reporter gene, transfection efficiency was standardized by adding 80 ng per well of the *Renilla* luciferase (RLUC) reporter vector phRL-TK (Promega) to the transfection mixture. Cell lysis and quantification of FLUC and RLUC activities on a BiotekFLx800 luminometer were performed using the Dual-Luciferase reporter assay system (Promega) according to the manufacturer's instructions. For each sample, FLUC activity was normalized against RLUC activity.

CAT activity was determined following a previously described protocol (39). Reaction products were analyzed by ascending thin-layer chromatography developed with 19:1 chloroform:methanol followed by autoradiography. CAT activity was calculated by determining the percentage of monoacetylated chloramphenicol species relative to total counts.

Purification and analysis of RNA by Northern blotting. Transfected cell monolayers were lysed at the indicated times with TRIzol reagent (Thermo Fisher), and total RNA was extracted according to the manufacturer's instructions. To purify CAT mRNA, cells were lysed in TNEN (50 mM Tris [pH 7.4], 150 mM NaCl, 1 mM EDTA, 0.5 mM dithiothreitol, 0.2% Nonidet P-40), the cytoplasmic fraction was recovered after centrifugation, and capped mRNAs were immunoselected with protein A-Sepharose beads using monoclonal anti-cap antibody H-20, as indicated previously (39, 41).

Purified total RNA (10^5 cells per lane) was resolved on 1.5% agarose-morpholinepropanesulfonic acid gels containing 2.2 M formaldehyde. At the end of the run, ribosomal RNAs were UV-visualized upon gel staining with ethidium bromide. The RNA was transferred onto a Hybond-N membrane (GE Healthcare, Amersham) as indicated by the manufacturer. Blots were probed with a CAT riboprobe that was synthesized by *in vitro* transcription of a linearized pGEMCAT, using T7 polymerase and [α-^{32}P]CTP, as previously described (39). Filters were exposed to film (BioMax film; Kodak) with an intensifying screen at −70°C.

Reverse transcription and real-time PCR. Aliquots of capped mRNAs were reverse transcribed with SuperScript II reverse transcriptase, according to the manufacturer's instructions (Thermo Fisher Scientific), using primers specific for CAT (CATqr, 5′-GCCAATCCCTGGGTGAGTTT-3′) and glyceraldehyde-3-phosphate dehydrogenase (GAPDHqr, 5′-CAGAAGGTGCGGAGATGATGA-3′) housekeeping gene. Amplification of a CAT or GAPDH 110-bp DNA fragment was carried out with oligonucleotides designed by using Primer Express software v3.0.1 (Applied Biosystems). Real-time PCRs were run in triplicate, using a 1/40 dilution of cDNA, 300 nmol of each primer (CATqf, 5′-ACCTTGTCGCCTTGCGTATAA-3′ and CATqr or GAPDHqf, 5′-TGCTGGTGCCGAGTATGTTG-3′, and GAPDHqr), and 10 μL of 2× FastStart Universal SYBR green master mix (Rox; Roche) in a final volume of 20 μL. PCR cycle conditions were set as follows: preincubation for 10 min at 95°C, followed by 40 cycles, each including 15 s at 95°C and 60 s at 60°C. Dissociation curves were generated at the end of the run to verify the specificity of the reaction product. Relative quantification was performed by using Applied Biosystems 7500 real-time PCR software v2.0.6 (Thermo Fisher Scientific). Average cycle threshold (C_T) values for FLUC were normalized to the average C_T values for GAPDH, and the relative CAT RNA content was estimated as the $\Delta\Delta C_T$-based fold change.

Mouse infection. The rTCRV virulence study in newborn mice was conducted in biosafety level 3 facilities at the Instituto Nacional de Enfermedades Virales Humanas "Dr. Julio I. Maiztegui" (INEVH, Pergamino, Argentina). Study sample sizes in the animal experiment were chosen based on experience in our labs with respect to group sizes readily revealing biologically significant differences in the experimental model used.

Groups of 10 mice (2-day-old BALB/cJ mice) were injected intracranially with 1, 10, 10^2, or 10^3 PFU/animal of wild-type rTCRV or rTCRVsNCR. Groups of animals (n = 10) were inoculated with medium as negative controls or left uninfected for environmental controls. Mice were monitored daily over a 21-day

period. Two mice per group were sacrificed at day 8 postinoculation, and brains, spleens, and livers were collected for determination of viral titers by plaque assay on Vero cells. Endpoint survivor animals were humanely euthanized.

Ethics statement. The virulence study in mice was carried out according to the INEVH ethics manual, *Guide for the Use and Care of Experimental Animals*, under protocol number 10670/2021.

Statistics. Statistical analyses were performed using GraphPad software. Statistical significance in Fig. 1 to 4 was assessed using a one-way analysis of variance (ANOVA) with Bonferroni's multiple-comparison test, with a confidence interval of >95%. Data are presented as means ± standard deviations (SD). For statistical analysis of viral growth curves (Fig. 5), viral titer values were log-transformed and a multiple *t* test for each day along the curve was run. A multiple *t* test was also employed to analyze viral load in brain tissue from inoculated mice (Fig. 6B). Mouse survival curves were compared with log-rank (Mantel-Haenszel) and Gehan-Breslow-Wilcoxon tests (data not shown). Levels of significance are indicated by asterisks: *, $P \leq 0.05$; **, $P \leq 0.01$; ***, $P \leq 0.001$; ****, $P \leq 0.0001$. Unless otherwise specified, all experiments were repeated at least three times.

ACKNOWLEDGMENTS

We are grateful to Sabrina Foscaldi for technical contributions and helpful discussions. We also thank Agustina Gallo (INTA, Mendoza, Argentina) for assistance with statistical analysis. The technical aid of J. Acevedo and S. Rojana (CEVHAN) is acknowledged.

This work was supported by Agencia Nacional de Promoción Científica y Tecnológica (ANPCyT) and CONICET. A.D., C.S., and N.L. are research investigators of CONICET. G.L.G. received a fellowship from CONICET.

REFERENCES

1. Radoshitzky SR, Buchmeier MJ, Charrel RN, Clegg JCS, Gonzalez J-PJ, Günther S, Hepojoki J, Kuhn JH, Lukashevich IS, Romanowski V, Salvato MS, Sironi M, Stenglein MD, de la Torre JC, ICTV Report Consortium. 2019. ICTV Virus Taxonomy Profile: Arenaviridae. J Gen Virol 100:1200–1201. https://doi.org/10.1099/jgv.0.001280.
2. Downs WG, Anderson CR, Spence L, Aitken THG, Greenhall AH. 1963. Tacaribe virus, a new agent isolated from Artibeus bats and mosquitoes in Trinidad, West Indies. Am J Trop Med Hyg 12:640–646. https://doi.org/10.4269/ajtmh.1963.12.640.
3. Sayler KA, Barbet AF, Chamberlain C, Clapp WL, Alleman R, Loeb JC, Lednicky JA. 2014. Isolation of Tacaribe virus, a Caribbean arenavirus, from host-seeking Amblyomma americanum ticks in Florida. PLoS One 9:e115769. https://doi.org/10.1371/journal.pone.0115769.
4. Maes P, Alkhovsky SV, Bào Y, Beer M, Birkhead M, Briese T, Buchmeier MJ, Calisher CH, Charrel RN, Choi IR, Clegg CS, de la Torre JC, Delwart E, DeRisi JL, Di Bello PL, Di Serio F, Digiaro M, Dolja VV, Drosten C, Druciarek TZ, Du J, Ebihara H, Elbeaino T, Gergerich RC, Gillis AN, Gonzalez J-PJ, Haenni A-L, Hepojoki J, Hetzel U, Hồ T, Hóng N, Jain RK, Jansen van Vuren P, Jin Q, Jonson MG, Junglen S, Keller KE, Kemp A, Kipar A, Kondov NO, Koonin EV, Kormelink R, Korzyukov Y, Krupovic M, Lambert AJ, Laney AG, LeBreton M, Lukashevich IS, Marklewitz M, Markotter W, et al. 2018. Taxonomy of the family Arenaviridae and the order Bunyavirales: update 2018. Arch Virol 163:2295–2310. https://doi.org/10.1007/s00705-018-3843-5.
5. Brisse ME, Ly H. 2019. Hemorrhagic fever-causing arenaviruses: lethal pathogens and potent immune suppressors. Front Immunol 10:372. https://doi.org/10.3389/fimmu.2019.00372.
6. Martínez-Peralta LA, Coto CE, Weissenbacher MC. 1993. The Tacaribe complex: the close relationship between a pathogenic (Junin) anda non-pathogenic (Tacaribe) arenavirus, p 281–296. *In* Salvato MS (ed), The Arenaviridae. Plenum Press, New York, NY.
7. Franze-Fernández MT, Iapalucci S, López N, Rossi C. 1993. Subgenomic RNAs of Tacaribe virus, p 113–132. *In* Salvato MS (ed), The Arenaviridae. Plenum Press, New York, NY.
8. Buchmeier MJ. 2007. Arenaviridae: the viruses and their replication, p 1791–1827. *In* Knipe DM, Howley PM, Griffin DE, Lamb RA, Martin MA (ed), Fields Virology, 5th ed. Lippincott Williams & Wilkins, Philadelphia, PA.
9. López N, Franze-Fernández MT. 2007. A single stem-loop structure in Tacaribe arenavirus intergenic region is essential for transcription termination but is not required for a correct initiation of transcription and replication. Virus Res 124:237–244. https://doi.org/10.1016/j.virusres.2006.10.007.
10. Raju R, Raju L, Hacker D, Garcin D, Compans R, Kolakofsky D. 1990. Nontemplated bases at the 5′ ends of Tacaribe virus mRNAs. Virology 174:53–59. https://doi.org/10.1016/0042-6822(90)90053-t.
11. Morin B, Coutard B, Lelke M, Ferron F, Kerber R, Jamal S, Frangeul A, Baronti C, Charrel R, de Lamballerie X, Vonrhein C, Lescar J, Bricogne G, Günther S, Canard B. 2010. The N-terminal domain of the arenavirus L protein is an RNA endonuclease essential in mRNA transcription. PLoS Pathog 6:e1001038. https://doi.org/10.1371/journal.ppat.1001038.
12. Iapalucci S, López N, Franze-Fernández MT. 1991. The 3′ end termini of the Tacaribe arenavirus subgenomic RNAs. Virology 182:269–278. https://doi.org/10.1016/0042-6822(91)90670-7.
13. Franze-Fernández MT, Zetina C, Iapalucci S, Lucero MA, Bouissou C, López R, Rey O, Daheli M, Cohen GN, Zakin MM. 1987. Molecular structure and early events in the replication of Tacaribe arenavirus S RNA. Virus Res 7:309–324. https://doi.org/10.1016/0168-1702(87)90045-1.
14. King BR, Samacoits A, Eisenhauer PL, Ziegler CM, Bruce EA, Zenklusen D, Zimmer C, Mueller F, Botten J. 2018. Visualization of arenavirus RNA species in individual cells by single-molecule fluorescence *in situ* hybridization suggests a model of cyclical infection and clearance during persistence. J Virol 92. https://doi.org/10.1128/JVI.02241-17.
15. Meyer BJ, de la Torre JC, Southern PJ. 2002. Arenaviruses: genomic RNAs, transcription, and replication. Curr Top Microbiol Immunol 262:139–157. https://doi.org/10.1007/978-3-642-56029-3_6.
16. Vogel D, Rosenthal M, Gogrefe N, Reindl S, Günther S. 2019. Biochemical characterization of the Lassa virus L protein. J Biol Chem 294:8088–8100. https://doi.org/10.1074/jbc.RA118.006973.
17. Kolakofsky D, Garcin D. 1993. The unusual mechanism of arenavirus RNA synthesis, p 103–112. *In* Salvato MS (ed), The Arenaviridae. Plenum Press, New York, NY.
18. Hass M, Westerkofsky M, Müller S, Becker-Ziaja B, Busch C, Günther S. 2006. Mutational analysis of the Lassa virus promoter. J Virol 80:12414–12419. https://doi.org/10.1128/JVI.01374-06.
19. Perez M, de la Torre JC. 2003. Characterization of the genomic promoter of the prototypic arenavirus lymphocytic choriomeningitis virus. J Virol 77:1184–1194. https://doi.org/10.1128/jvi.77.2.1184-1194.2003.
20. Kranzusch PJ, Schenk AD, Rahmeh AA, Radoshitzky SR, Bavari S, Walz T, Whelan SPJ. 2010. Assembly of a functional Machupo virus polymerase complex. Proc Natl Acad Sci U S A 107:20069–20074. https://doi.org/10.1073/pnas.1007152107.
21. Peng R, Xu X, Jing J, Wang M, Peng Q, Liu S, Wu Y, Bao X, Wang P, Qi J, Gao GF, Shi Y. 2020. Structural insight into arenavirus replication machinery. Nature 579:615–619. https://doi.org/10.1038/s41586-020-2114-2.
22. Kouba T, Vogel D, Thorkelsson SR, Quemin ERJ, Williams HM, Milewski M, Busch C, Günther S, Grünewald K, Rosenthal M, Cusack S. 2021. Conformational changes in Lassa virus L protein associated with promoter binding and RNA synthesis activity. Nat Commun 12:7018. https://doi.org/10.1038/s41467-021-27305-5.
23. Casabona JC, Levingston Macleod JM, Loureiro ME, Gomez GA, Lopez N. 2009. The RING domain and the L79 residue of Z protein are involved in both the rescue of nucleocapsids and the incorporation of glycoproteins

into infectious chimeric arenavirus-like particles. J Virol 83:7029–7039. https://doi.org/10.1128/JVI.00329-09.
24. Foscaldi S, Loureiro ME, Sepúlveda C, Palacios C, Forlenza MB, López N. 2020. Development of a reverse genetic system to generate recombinant chimeric Tacaribe virus that expresses Junín virus glycoproteins. Pathogens 9:948. https://doi.org/10.3390/pathogens9110948.
25. Taniguchi S, Yoshikawa T, Shimojima M, Fukushi S, Kurosu T, Tani H, Fukuma A, Kato F, Nakayama E, Maeki T, Tajima S, Lim C-K, Ebihara H, Kyuwa S, Morikawa S, Saijo M. 2020. Analysis of the function of the lymphocytic choriomeningitis virus S segment untranslated region on growth capacity in vitro and on virulence in vivo. Viruses 12:896. https://doi.org/10.3390/v12080896.
26. Albariño CG, Bird BH, Chakrabarti AK, Dodd KA, Erickson BR, Nichol ST. 2011. Efficient rescue of recombinant Lassa virus reveals the influence of S segment noncoding regions on virus replication and virulence. J Virol 85:4020–4024. https://doi.org/10.1128/JVI.02556-10.
27. Pflug A, Guilligay D, Reich S, Cusack S. 2014. Structure of influenza A polymerase bound to the viral RNA promoter. Nature 516:355–360. https://doi.org/10.1038/nature14008.
28. Gerlach P, Malet H, Cusack S, Reguera J. 2015. Structural insights into Bunyavirus replication and its regulation by the vRNA promoter. Cell 161:1267–1279. https://doi.org/10.1016/j.cell.2015.05.006.
29. Te Velthuis AJW, Grimes JM, Fodor E. 2021. Structural insights into RNA polymerases of negative-sense RNA viruses. Nat Rev Microbiol 19:303–318. https://doi.org/10.1038/s41579-020-00501-8.
30. Pyle JD, Whelan SPJ. 2019. RNA ligands activate the Machupo virus polymerase and guide promoter usage. Proc Natl Acad Sci U S A 116:10518–10524. https://doi.org/10.1073/pnas.1900790116.
31. Ye C, de la Torre JC, Martinez-Sobrido L. 2020. Reverse genetics approaches for the development of mammarenavirus live-attenuated vaccines. Curr Opin Virol 44:66–72. https://doi.org/10.1016/j.coviro.2020.06.011.
32. Fuller-Pace FV, Southern PJ. 1988. Temporal analysis of transcription and replication during acute infection with lymphocytic choriomeningitis virus. Virology 162:260–263. https://doi.org/10.1016/0042-6822(88)90419-9.
33. Haist K, Ziegler C, Botten J. 2015. Strand-specific quantitative reverse transcription-polymerase chain reaction assay for measurement of arenavirus genomic and antigenomic RNAs. PLoS ONE 10:e0120043. https://doi.org/10.1371/journal.pone.0120043.
34. Romanowski V. 1993. Genetic organization of Junin virus, the etiological agent of Argentine hemorrhagic fever, p 51–83. *In* Salvato MS (ed), The Arenaviridae. Plenum Press, New York, NY.
35. Iapalucci S, Cherñavsky A, Rossi C, Burgín MJ, Franze-Fernández MT. 1994. Tacaribe virus gene expression in cytopathic and non-cytopathic infections. Virology 200:613–622. https://doi.org/10.1006/viro.1994.1224.
36. Ito N, Takayama-Ito M, Yamada K, Hosokawa J, Sugiyama M, Minamoto N. 2003. Improved recovery of rabies virus from cloned cDNA using a vaccinia virus-free reverse genetics system. Microbiol Immunol 47:613–617. https://doi.org/10.1111/j.1348-0421.2003.tb03424.x.
37. López R, Franze-Fernández MT. 1985. Effect of Tacaribe virus infection on host cell protein and nucleic acid synthesis. J Gen Virol 66:1753–1761. https://doi.org/10.1099/0022-1317-66-8-1753.
38. D'Antuono A, Loureiro ME, Foscaldi S, Marino-Buslje C, Lopez N. 2014. Differential contributions of Tacaribe arenavirus nucleoprotein N-terminal and C-terminal residues to nucleocapsid functional activity. J Virol 88:6492–6505. https://doi.org/10.1128/JVI.00321-14.
39. López N, Jácamo R, Franze-Fernández MT. 2001. Transcription and RNA replication of Tacaribe virus genome and antigenome analogs require N and L proteins: Z protein is an inhibitor of these processes. J Virol 75:12241–12251. https://doi.org/10.1128/JVI.75.24.12241-12251.2001.
40. Radecke F, Spielhofer P, Schneider H, Kaelin K, Huber M, Dötsch C, Christiansen G, Billeter MA. 1995. Rescue of measles viruses from cloned DNA. EMBO J 14:5773–5784. https://doi.org/10.1002/j.1460-2075.1995.tb00266.x.
41. Bochnig P, Reuter R, Bringmann P, Luhrmann R. 1987. A monoclonal antibody against 2,2,7-trimethylguanosine that reacts with intact, class U, small nuclear ribonucleoproteins as well as with 7-methylguanosine-capped RNAs. Eur J Biochem 168:461–467. https://doi.org/10.1111/j.1432-1033.1987.tb13439.x.